Auditory brainstem responses in the nine-banded armadillo (*Dasypus novemcinctus*)

Thomas Brad Moffitt[1], Samuel Atcherson[2] and Jeffrey Padberg[1]

[1] Biology, University of Central Arkansas, Conway, AR, USA
[2] Department of Audiology and Speech Pathology, University of Arkansas for Medical Sciences, Little Rock, AR, United States

ABSTRACT

The auditory brainstem response (ABR) to tone burst stimuli of thirteen frequencies ranging from 0.5 to 48 kHz was recorded in the nine-banded armadillo (*Dasypus novemcinctus*), the only extant member of the placental mammal superorder Xenarthra in North America. The armadillo ABR consisted of five main peaks that were visible within the first 10 ms when stimuli were presented at high intensities. The latency of peak I of the armadillo ABR increased as stimulus intensity decreased by an average of 20 µs/dB. Estimated frequency-specific thresholds identified by the ABR were used to construct an estimate of the armadillo audiogram describing the mean thresholds of the eight animals tested. The majority of animals tested (six out of eight) exhibited clear responses to stimuli from 0.5 to 38 kHz, and two animals exhibited responses to stimuli of 48 kHz. Across all cases, the lowest thresholds were observed for frequencies from 8 to 12 kHz. Overall, we observed that the armadillo estimated audiogram bears a similar pattern as those observed using ABR in members of other mammalian clades, including marsupials and later-derived placental mammals.

INTRODUCTION

The nine-banded armadillo (*Dasypus novemcinctus*) is the only extant North American member of superclade Xenarthra, a relatively early-derived clade of placental mammals that includes the extant sloths, anteaters, and armadillos (*e.g.*, *Delsuc et al., 2002*; *Gaudin, 2003*; *Morgan et al., 2013*). Xenarthrans are thought to have originated in the South American continent approximately 58 million years ago and spread into North America along the Isthmus of Panama, becoming widespread and diverse during the Neogene period (*Scillato-Yané, 1976*; *Oliveira & Bergqvist, 1998*; *Bergqvist, Abrantes & Avilla, 2004*; *Moller-Krull et al., 2007*; *Webb, 1976*; *Stehli & Webb, 1985*; *Vizcaino, Bargo & Farina, 2008*; also reviewed in *Padberg, 2017*). During the Pleistocene, North American xenarthrans went extinct, and diversity in the remaining members of the clade decreased (*Delsuc, Vizcaíno & Douzery, 2004*; for review, see *Vizcaíno & Bargo, 2014*; *Moraes-Barros & Arteaga, 2015*). Of the thirty-nine extant xenathran species, all are endemic to South

Corresponding author
Jeffrey Padberg, jpadberg@uca.edu

and/or Central America with the exception of nine-banded armadillos, whose range includes a large portion of South, Central, and North America and continues to expand in the United States (*e.g.*, *Loughry et al., 2013*; *Superina & Loughry, 2015*).

Historically, nine-banded armadillos have been used as a model for Hansen's disease research (*e.g.*, *Kirchheimer & Storrs, 1971*; *Truman et al., 2011*; *Sharma et al., 2015*; for review, see *Sharma et al., 2013*) or studies of reproductive physiology and development due to their polyembryonic reproduction in which every litter is composed of four identical quadruplets resulting from a single fertilized egg (*e.g.*, *Loughry et al., 1998*, *2015*). Less is known about the sensory systems of this species aside from relatively coarse characterizations of the sensory and motor cortical areas (*Dom et al., 1971*; *Royce & Martin, 1975*). Recently, renewed interest in characterizing the neural systems of this species has emerged, with a focus on examining the evolution of sensory and motor specializations in xenarthrans, including features such as photoreceptor arrays, orientation selectivity in neurons in primary visual cortex, and transcriptomic organization of motor cortices (*Emerling & Springer, 2015*; *Scholl et al., 2017*; *Yanny et al., 2021*; *Wirthlin et al., 2023*).

With regard to the auditory system, a relatively large extent of electrophysiologically— defined auditory cortex compared to other sensory regions has been described in the brain of the nine-banded armadillo (*Royce & Martin, 1975*). The inferior colliculi are large, protruding above the midbrain in dasypoid armadillos (*e.g.*, *Ferrari, 1998*), and a proportionally large subcortical auditory system is observed in armadillos compared to those of many other mammals (*e.g.*, *Glendenning & Masterton, 1998*). Nine-banded armadillos also have large, highly mobile pinnae.

Some aspects of auditory function (frequency range, mean maximum sensitivity, and spectral region of maximum sensitivity) in a few xenarthran species including *Dasypus novemcinctus* have been measured using cochlear microphonic (CM) techniques (*Suga, 1967*; *Peterson & Heaton, 1968*). The functional organization of sensory areas including auditory cortex in armadillos has also been examined using evoked potentials from recordings on the cortical surface (*Royce & Martin, 1975*). The tonotopic organization of the auditory cortex was not examined, although its general caudolateral location on the hemisphere was determined based on evoked responses to a broadband auditory stimulus (the clicking sound of a camera shutter; *Royce & Martin, 1975*).

As part of a larger effort aimed at determining in detail the functional and anatomical organization of the auditory system in the armadillo, the goal of this study was to determine the frequency range and auditory sensitivity of *Dasypus novemcinctus* using estimated thresholds provided by ABR techniques. The noninvasive ABR has been used for decades to provide basic characterization of functions in the peripheral and central auditory system in a range of species (*e.g.*, *Jewett & Williston, 1971*; *Ridgway et al., 1981*; *Gorga et al., 1988*; *Reimer, 1995*, *1996*; *Cone-Wesson, Hill & Liu, 1997*; *Mills & Shepherd, 2001*; *Wilson & Mills, 2005*; *Atcherson & Stoody, 2012*; *Garrett et al., 2019*; *Tuebenbacher, Doss & Guevar, 2020*). Here we describe the morphology, amplitude, and thresholds of the ABR and present an audiogram for anesthetized *D. novemcinctus* based on estimated threshold levels for thirteen frequencies between 0.5 and 48 kHz.

Table 1 Mass and sex of armadillos in this study.

Case #	Sex	Mass (kg)
15–01	M	5.3
15–02	F	3.4
15–04	F	4.7
15–05	F	3.8
15–06	M	5.2
15–07	M	4.1
15–08	M	5.3
15–08	M	4.4

Note:
   Three female and five male armadillos were examined in this study, and weights and sex are shown.

MATERIALS AND METHODS

Eight wild-caught armadillos (three female, five male, weight 3.8–6 kg; Table 1) were used for this descriptive study. Ages were unknown, but based upon body size and weight all animals were estimated to be adults. The animals were housed in individual kennels containing corn cob or wood pellet substrate and soft paper bedding. Fresh water and food (Blue brand feline cat food mixed with Blue brand dog food and Vitalize Raw Max powder, supplemented by live earthworms) were provided daily. The quarters were maintained at 22 °C with a 12 h day/night lighting cycle.

Animals were anesthetized by isoflurane (1.75–2.5%) delivered *via* nose mask. Once the animals were unresponsive, the skin of the head and dorsal neck was disinfected with 70% ethanol, 4% chlorhexidine gluconate surgical scrub, and sterile stainless steel needle electrodes (Natus Neurology Inc, Warwick, RI, USA) were placed subdermally at the back of the neck (ground), behind the ear (inverting), and cheek (non-inverting; Fig. 1). These positions for the electrodes were chosen to avoid the cephalic shield, the bony plate on the dorsal portion of the armadillo head. The pinna and the ear canal were visually examined to determine they were clear of any obstructions, and a hollow tube with a form-fitting foam tip was placed into the ear canal for stimulus delivery. At the conclusion of each recording session, the anesthesia was withdrawn and once alert, the animals were returned to their home cages. All procedures were approved by the Institutional Animal Care and Use Committee at the University of Central Arkansas (Approval #13-003; UCA PHS (Public Health Service) Animal Welfare Assurance #A4179-01) and followed USDA and NIH guidelines.

To first identify and characterize the physiological ABR response, 50 μs broadband clicks were presented at a rate of 27.7/s and at peak-to-peak equivalent sound pressure levels (peSPL) of 100 dB and lower using a clinical Bio-Logic Navigator Pro system (Natus Neurology Inc. Warwick, RI). Next, tone burst stimuli with 2 ms rise-plateau-fall times (6 ms total duration) were presented at a stimulation rate of 27.7/s from 0.5 to 48 kHz with 13 frequencies of 0.5, 1, 2, 4, 8, 12, 16, 20, 25, 32, 38, 44, and 48 kHz. Stimuli between 0.5 and 2 kHz were generated by a Bio-Logic Navigator Pro system (Natus Neurology Inc.,
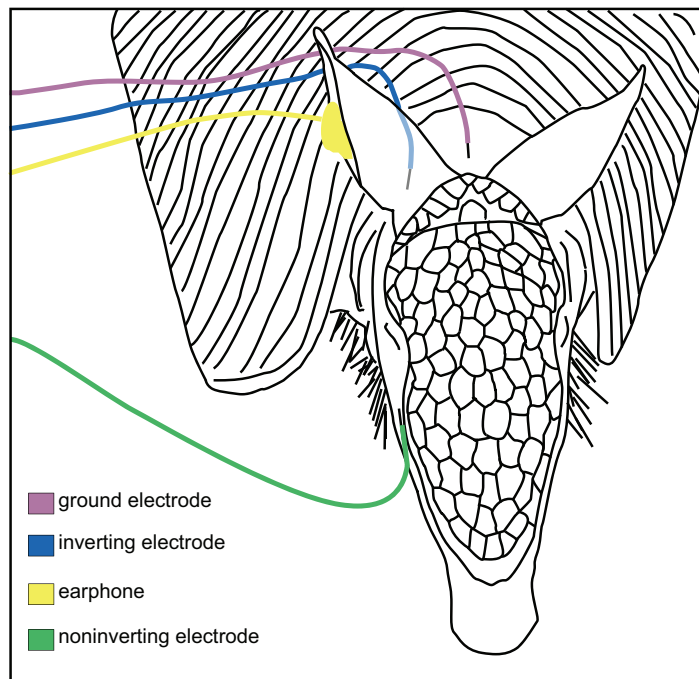
Figure 1 Placement of electrodes on the armadillo head. Placement of subdermal needle electrodes on anesthetized armadillo during ABR experiments using right ear. Noninverting electrode (green) was placed on the snout just lateral to cephalic shield, inverting electrode (blue) was placed immediately caudal to pinna, and ground electrode (rose) was placed along the midline of the dorsal neck. A hollow tube from the transducer was tipped with a form-fitting earplug to fit into the ear canal (yellow). Positions of electrodes and earphone were mirrored for testing the left ear. Adapted from *Moffitt (2015)*.

Warwick, RI, USA), which also served as the evoked potential recording system for all responses in this study.

All remaining stimuli (4 kHz and higher) were generated by Spike2 software *via* a linked CED 3505 programmable attenuator, ED-1 speaker driver (Cambridge Electronic Design, Cambridge, UK), and EC-1 transducer (Tucker Davis Technologies, Alachua, FL, USA) with a time-locked trigger sent to the connected Navigator Pro evoked potential system. Peak-to-peak equivalent sound pressure levels (pe SPL) of each tone burst was measured using a Type 2250 sound level meter (Brüel & Kjær, Duluth, GA, USA) coupled to an oscilloscope and checked against the peak-to-peak value of a 94 dB SPL reference tone at 1 kHz using a Type 4231 piston phone (Brüel & Kjær, Duluth, GA, USA; Table 2).

All recordings were bandpass filtered 30 to 1,500 Hz and collected within a 16 ms time window. Recordings were collected and averaged online until the peakform had stabilized (typically 1,000–1,200 sweeps). ABRs were collected starting with maximum output levels, and intensities were then decreased by 10 dB in successive trials until no visually identifiable response could be measured (Table 2). Thresholds were defined by the lowest stimulus level as follows: (1) at least two repeated responses, (2) a minimum peak I amplitude that is equal to twice the level of the maximum background response, and (3) confirmed by two trained observers. The threshold values were then compiled into Excel

Table 2 Minimum and mean ABR thresholds and maximum stimulus levels by frequency.

Frequency	Number of responsive animals/tested	Minimum threshold peSPL (dB)	Mean threshold peSPL (dB)	Standard deviation	Maximum stimulus level peSPL (dB)
0.5 kHZ	6/6	79.9	87.0	5.45	95.0
1 kHz	7/7	69.6	77.6	6.41	94.6
2 kHz	7/7	51.8	66.9	9.62	106.8
4 kHz	8/8	27.7	37.4	7.96	72.7
8 kHz	8/8	1.8	26.1	13.14	69.3
12 kHz	8/8	4.7	23.5	15.40	67.2
16 kHz	8/8	13.1	33.3	14.12	68.1
20 kHz	8/8	26.8	40.2	11.35	71.8
25 kHz	7/7	37	52.4	14.29	77.0
32 kHz	6/8	28.5	43.9	10.31	63.5
38 kHz	4/6	34.7	49.1	12.81	67.2
44 kHz	1/6	38.7	38.7	–	61.2
48 kHz	2/5	30.3	39.1	12.01	52.8

Note:
Numbers of animals tested and responsive for the frequencies between 0.5 and 48 kHz, with minimum, mean thresholds, standard deviations, and maximum stimulus level for each frequency.

(Microsoft, Redmond, WA) to generate descriptive statistics. To assess any potential effects of sex on thresholds across the tested frequencies, we conducted a two-way mixed model ANOVA with frequency as a within-cases variable and sex as a between-groups variable (IBM SPSS Statistics for Windows, version 27 (IBM Corp., Armonk, N.Y., USA)).

RESULTS

ABR morphology

The armadillo ABR to broadband clicks at high stimulus intensities (>65 dB) consisted of five peaks between the first 1–5 ms after stimulus onset (Fig. 2). Within the first millisecond after stimulation at intensities greater than 60 dB, and prior to the first peak, evidence of the cochlear microphonic was also observed in the waveform. Peak I was present within the first two milliseconds at high stimulus intensity. The second peak was visible following a deep trough after peak I. The third peak had a relatively high amplitude, and was followed closely by peak IV. The smaller fifth peak was evident within approximately four milliseconds post stimulus and was only observed at relatively high stimulus intensities.

The armadillo ABR to tone bursts consisted of up to four peaks within the first 6 ms, followed by a large negative deflection from approximately 6–9 ms (Fig. 3). This negative deflection was most obvious at higher stimulus intensities, and as the intensity of the stimulus was lowered the slope of the negative trend also decreased. Within approximately 20 dB of threshold intensity for each frequency the negative deflection became indistinguishable from background. In contrast to the ABR observed with broadband clicks, peak II was typically absent in responses to tone burst stimuli.
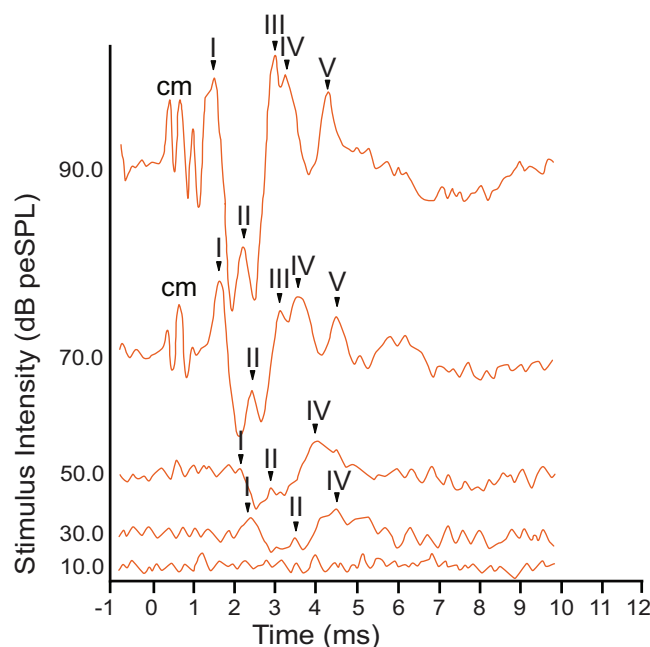
Figure 2 Representative ABR peakform in response to broadband clicks. Representative ABR peakform morphology in response to broadband clicks of alternating polarity stimuli at intensities between 10–90 dB peSPL. At high stimulus intensities (>65 dB peSPL), cochlear microphonic response was evident within 1 ms after stimulation. Peaks I–V were observed in the first 5 ms after stimulation. In all cases, peak I was consistently the peak with highest amplitude and was the most reliably observed peak across all stimulus levels.
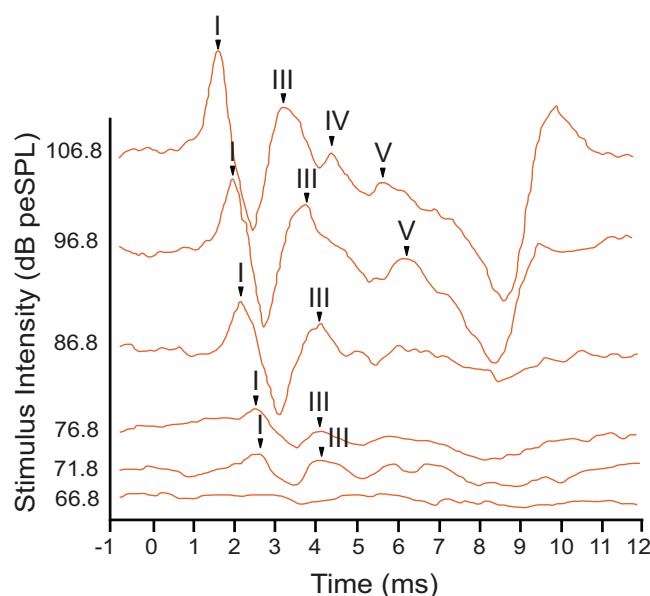
Figure 3 Representative ABR peakform in response to toneburst stimuli. ABR peakform morphology in response to 2 kHz tone burst alternating polarity stimuli at intensities between 65–107 dB peSPL. Stimuli were presented to the left ear at a rate of 27.7 repetitions per second. At highest stimulus intensities, four peaks (I–V) were present, and a negative trend following peak V was evident approximately 7 ms after stimulation. The overall morphology of the peakform changed as stimulus intensity was lowered. As observed with click stimuli, peak 1 consistently had the highest amplitude and was the most reliably observed peak across all tone burst stimulus levels.
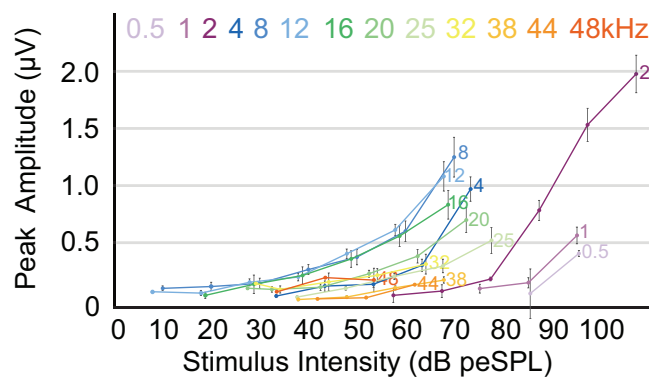
Figure 4 ABR amplitude across selected frequencies. Input-output function of the peak 1 amplitudes for all frequencies tested. Peak amplitudes for all frequencies increased with stimulus intensities. Frequencies are indicated at the right side of the corresponding line. Error bars at each data point indicate mean ± SEM values ($n = 6$ for 0.5 Hz, $n = 7$ for 1 and 2 kHz; $n = 8$ for 4, 8, 12, 16, and 20 kHz; $n = 7$ for 25 kHz, $n = 6$ for 32 kHz; $n = 4$ for 38 kHz, $n = 1$ for 44 kHz, and $n = 2$ for 48 kHz).

In response to tone bursts, peak I, the neural signal generated by activity in the cochlear nucleus, consistently had the highest amplitude with a maximum of 2.46 µV, and this peak was present at all stimulus levels where a response was observed for each frequency. Response amplitudes decreased as stimuli were attenuated, until later peaks became indistinguishable from the background while peak I and III remained visible. This pattern was consistent for all animals tested, and for all frequencies presented. Due to the reliability of peak I, all amplitude and latency measurements were made using this peak. Peak III was frequently the last peak to remain visible above background, but was not reliably observed across all frequencies or intensities.

ABR amplitude and latency

The highest amplitude of peak I during unattenuated stimuli varied depending on frequency (Fig. 4). Amplitude of peak I during the lowest frequency stimulus (0.5 kHz) averaged 0.44 µV, and as the frequencies increased the peak amplitude of peak I also increased until 2 kHz, at which the maximum amplitude of 1.97 µV was observed. From 4 to 12 kHz, peak amplitudes were relatively stable, but declined from 12 through 48 kHz. The latency of peak I was similar between the animals in this study and between recording sessions for unattenuated stimuli of the same frequency. Most frequencies tested showed similar peak I latencies, indeed, latencies for nine of the 13 frequencies were within 10 percent of each other (Fig. 5). Unattenuated latencies were longest at the highest frequency tested (48 kHz) and at the lowest frequency tested (0.5 kHz), with mean values of 4.64 and 3.56 ms, respectively. For nearly all frequencies, as stimulus intensities were reduced, latencies increased.

ABR threshold

The audiogram was constructed using the mean threshold level at each frequency from all animals tested (Table 2). The 0.5 kHz stimulus was tested on six animals, and five of those exhibited clear responses. ABR responses were reliably obtained from stimuli ranging from
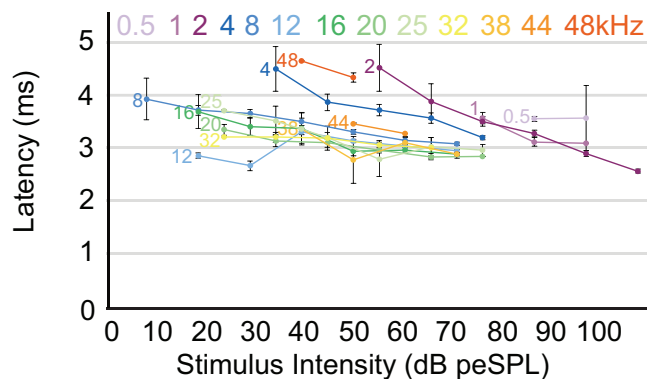
Figure 5 Latency/intensity function for armadillo ABR. Mean latency of wave I as a function of stimulus intensity. Latency/intensity relationships show an average of 0.018 ms increase per dB of attenuation. Stimuli from 0.5–4 kHz had an average latency increase of 0.034 ms per dB of attenuation, while frequencies above 4 kHz had an average latency increase of 0.013 ms per dB of attenuation. Frequencies are indicated at the start of each corresponding line. Error bars indicate SEM values.
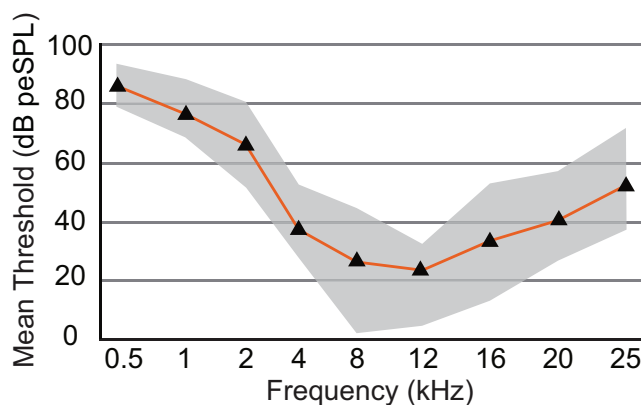
Figure 6 Audiogram of ABR-derived thresholds for *Dasypus novemcinctus*. Audiogram of *D. novemcinctus* estimated from mean ABR thresholds in the current study. Area of greatest sensitivity in armadillos is from 8 to 12 kHz. Maximum and minimum threshold values observed for each frequency are indicated in grey shading. Six to eight animals were tested for each frequency, and all animals were responsive at all frequencies between 0.5 and 25 kHz. At frequencies of 32, 38, 44, and 48 kHz, not all animals were responsive and data are not shown (see Table 2). The lowest mean and minimum thresholds were observed at 8 kHz (26.1 and 1.8 dB peSPL respectively) and 12 kHz (23.5 and 4.7 dB peSPL respectively).

0.5 to 25 kHz in all animals tested, and the lowest thresholds were observed from 8 to 12 kHz (1.8 and 4.7 dB, respectively; Fig. 6). As stimuli from 32 to 48 kHz were less reliable in invoking a response with six of eight animals showing responses to 32 kHz, four of six animals responding to 38 kHz, one of six responding to 44 kHz, and two of five animals responding to 48 kHz, these thresholds are not included in Fig. 6. The audiogram obtained from mean threshold levels is similar in morphology to that obtained from many other mammals which show a region of highest sensitivity towards the middle of the audiogram, and steep decreases in sensitivity in the lower and upper frequencies. The evoked responses in armadillos show a decrease from the region of highest sensitivity to the higher frequency
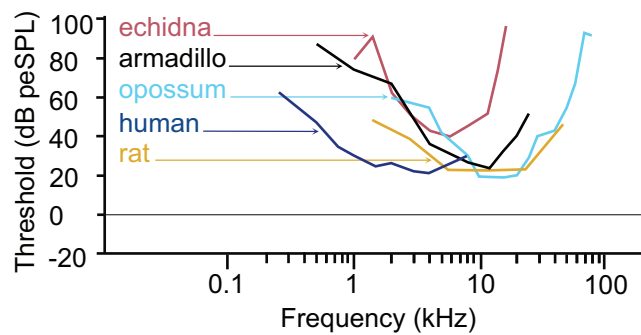
Figure 7 Comparative audiogram. Comparison of ABR-derived audiograms of several mammalian models on the log scale. The estimated threshold range of nine-banded armadillos is relatively wide, with lowest thresholds evident between 8 and 12 kHz. The armadillo audiogram based on the ABR is similar to that of the monotreme short beaked echidna, although the range of highest sensitivity is shifted slightly towards the higher frequencies. Note that different anesthetics were used in some species (human: awake, *Gorga et al., 1988*; echidna: ketamine/xylazine, *Mills & Shepherd, 2001*; armadillo: isoflurane, current study; rat: ketamine/xylazine, *Powers et al., 2006*; opossum: fluanisone/fentanyl citrate, *Reimer, 1995*). Thin lines with arrowheads point from species to the trace for that species (echidna–red, armadillo–black, opossum–light blue, human–dark blue, rat–goldenrod).

region of the audiogram and appear to plateau between 32 and 48 kHz. Potential effects of sex on auditory thresholds across the frequencies we tested was examined by conducting a two-way mixed model ANOVA with frequency as a within-cases variable and sex as a between-groups variable. There was no effect of sex ($F(1,6) = 1.385$, $p = 0.284$, $\eta_p^2 = 0.188$) nor any interaction ($F(4,24) = 1.71$, $p = 0.180$, $\eta_p^2 = 0.222$) between sex and the significant effect of frequency (($F(4,24) = 3.89$, $p = 0.014$, $\eta_p^2 = 0.394$); see Supplementary Materials; IBM SPSS Statistics for Windows, version 27 (IBM Corp., Armonk, N.Y., USA)).

DISCUSSION

The armadillo ABR to tone bursts consists of up to five peaks at higher stimulus intensities, and often only a single peak as the threshold level is approached. The auditory sensitivity increased sharply from 0.5 to 4 kHz, with the least sensitivity recorded at 0.5 kHz. The results of the present study suggest an auditory frequency range in nine-banded armadillos of 0.5 to 38 kHz. In all subjects, the highest sensitivity was observed between 8 to 12 kHz, with the lowest threshold observed at 8 kHz. The sensitivity to the higher frequencies (from 25 to 48 kHz) was comparatively reduced, with the majority of thresholds in this frequency range near 40 dB. Auditory brainstem responses to frequencies above 38 kHz were not reliably obtained in the current study, with only one case out of the eight tested responding to a 44 kHz stimulus, and two cases responding to 48 kHz. The armadillo audiogram based on ABR is consistent with what is observed in similar studies of representative species from other mammalian clades, including monotremes, marsupials, and eutherians (Fig. 7).

The pattern we observed in peak I latencies for frequencies between 8–12kHz in armadillos was generally flat, between 2.6 and 4 milliseconds, and was consistent with those described in other species. In humans, the lowest ABR thresholds were between 2–5 kHz, with latencies ranging between 7 and 13 ms for 2 kHz for peak V (*Gorga et al.,*

1988). The ABR elicited from pure tone bursts recorded from monotreme echidnas (*Tachyglossus aculeatus*) indicates lowest thresholds between 3 and 8 kHz, with relatively flat latencies between 9–18 ms (*Mills & Shepherd, 2001*). In marsupial opossums (*Monodelphis domestica*), the lowest thresholds were observed between 8–20 kHz with latencies centered around 2 ms for peak I (*Reimer, 1995*, *1996*). In rats, the lowest ABR thresholds were observed between 6–24kHz, with peak II latencies at approximately 3 ms (*Powers et al., 2006*). The marsupial tammar wallaby (*Macropus eugenii*) ABR revealed the lowest threshold between 8 and 16 kHz, with latencies between 3.2 and 4.2 ms (*Cone-Wesson, Hill & Liu, 1997*). In a recent study using ABR in fat-tailed dunnarts to determine estimate thresholds, the thresholds and latencies both decreased with increasing frequency, but frequencies above 47.5 kHz have not been described (*Garrett et al., 2019*).

The thresholds observed in our preparation in armadillos were similar to thresholds reported from ABR studies in other mammals (Fig. 7). It is important to note that ABR thresholds are generally higher than those derived from behavioral methods and may be more variable between subjects. Examination of studies of human subjects comparing directly comparing threshold measures between ABR and behavioral (psychophysical) methods have shown that ABR thresholds are typically 10–20 dB higher than those observed behaviorally (*e.g.*, *Gorga et al., 1988*; *Stapells, 2000*). Regardless, the ABR provides a relatively rapid way to estimate auditory function in animals without an extensive behavioral training regimen. Heffner and colleagues have used behavioral methods to generate audiograms for an extensive array of wild and domesticated mammals (*e.g.*, *Heffner, Heffner & Masterton, 1970*; *Heffner & Masterton, 1980*; *Heffner & Heffner, 1984*, *1990*, *2007*; *Heffner et al., 1994*; *Heffner, Koay & Heffner, 2020*; for review see *Heffner & Heffner, 2014*). Future behavioral studies in this species may further describe the characteristics of auditory functions of armadillos.

An earlier study using the cochlear microphonics method reported an upper frequency limit of 60 kHz in *Dasypus novemcinctus* (*Peterson & Heaton, 1968*), however, in the current study we were unable to test frequencies higher than 48 kHz due to limitations of our equipment. Our results indicate a region of maximum sensitivity between 8 and 12 kHz, which is a narrower band than that reported by *Peterson & Heaton (1968)*, who reported maximum sensitivity for this species between 3 and 25 kHz.

In many species, hearing sensitivity changes with age, with auditory thresholds tending to increase while the frequency range that the animal can detect decreases (*e.g.*, *Engle, Tinling & Recanzone, 2013*; for review, see: *Recanzone, 2018*; and *Keithley, 2019*). While we are unable to confirm whether this is true for armadillos because the animals used in this study were wild caught and thus their actual ages were unknown, we did examine any potential effects of sex on thresholds across the frequencies we tested. A two-way mixed model ANOVA with frequency as a within-cases variable and sex as a between-groups variable was performed. There was no significant difference in thresholds between male and female armadillos. We tested only three female animals and five males, and if there are subtle differences, it may not be evident in our study. A follow up study using captive-born animals with a known age and/or using larger numbers of animals of both sexes may be

helpful to determine the effects of age and sex on threshold levels and ability to detect frequencies at the more extreme ends of the audiogram in nine-banded armadillos.

It is established that high frequency hearing is important to localize sound sources (*e.g.*, *Masterton, Heffner & Ravizza, 1969*; *Heffner & Heffner, 2014*; *Heffner & Heffner, 2018*) and that animals with smaller heads typically rely more on higher frequencies to localize sound (for review see *Heffner & Heffner, 2008*. Factors such as functional interaural distance (*e.g.*, time between arrival of sound at each ear) and interaural intensity differences play a role (*Masterton, Heffner & Ravizza, 1969*; for review, see *Heffner & Heffner, 2018*). The armadillo has an interaural separation of approximately 2.5 cm, which should provide a functional interaural time difference of about 75 μs. In addition, the relatively large pinnae compared to their head size may help amplify sounds of interest as the pinnae are moved. It is unclear whether armadillos use both time and intensity cues, as these animals have not been tested in a behavioral paradigm. Interestingly, some fossorial species have lost the ability to detect high frequencies, as azimuthal orientation may be less relevant in an underground environment like a burrow (mole rat: *Bruns et al., 1988*; *Muller & Burda, 1989*; pocket gopher: *Heffner & Heffner, 1990*). The stem xenarthran may also have been fossorial (*e.g.*, *Simpson, 1931*; also see: *Emerling & Springer, 2015* for discussion); however, the data in the current study support that nine-banded armadillos retain the ability to detect high frequencies.

An important role of higher frequency hearing is to help direct the visual system to those sound sources (*e.g.*, *Heffner & Heffner, 1984*, *2018*). Although to date, the visual fields in this species are not described, armadillos have laterally placed eyes, are not known to have a visual streak in the retina (*St. Jules, 1984*), and do not have cone photoreceptors (*Emerling & Springer, 2015*). Thus, localization of the sound source to direct the eyes may be relatively limited in this species.

While ABR and behavioral studies can help determine the functional characteristics of mammalian auditory systems, recent advanced in molecular genetics are rapidly increasing our ability to examine gene expression in the brain. Molecular techniques including single nucleus transcriptomics have recently been used to compare neural structures across species (*Tosches & Laurent, 2019*; *Hodge et al., 2019*; *Kozlenkov et al., 2020*; *Bakken et al., 2021*). Future transcriptomic examination of the armadillo auditory cortex and thalamus may reveal whether specific genes thought to be critical for high frequency hearing (*e.g.*, *Shh* and *SK2*) are present in xenarthrans as they are in echolocators and other mammalian species (*e.g.*, *Teeling, Jones & Rossiter, 2016*; *Wang et al., 2021*; *Concas et al., 2021*).

CONCLUSIONS

Here we report for the first time the audiogram of the nine-banded armadillo using ABR methods. We observed that the nine-banded armadillos (*Dasypus novemcinctus*) in this study have a hearing range from 0.5 to 48 kHz, with best sensitivity in the range from 8 to 12 kHz. The audiogram for this species is the typical pattern observed in all mammalian species that have been examined using ABR. The current findings will be used for studies examining the tonotopic organization within the auditory cortex in armadillos. It would be of further interest to gather behavioral thresholds for auditory function in this species, as

well as examine how the hearing-related genes in this species may compare to members of other mammalian clades.

ACKNOWLEDGEMENTS

Special thanks to Drs. Barbara Clancy and Amrita Puri for helpful comments on the manuscript, to Dr. Mitch Sutter for helpful technical advice, and to Dr. Frank Knight for assistance with armadillos. Thanks to the Moffitt family for their encouragement. This article is dedicated to the enduring memory of Thomas (Brad) Moffitt, whom the world lost too soon.

Funding

This work was supported by the National Science Foundation (NSF IOS #1257891) to Jeffrey Padberg. The funders had no role in study design, data collection and analysis, decision to publish, or preparation of the manuscript.

Competing Interests

The authors declare that they have no competing interests.

Author Contributions

- Thomas Brad Moffitt performed the experiments, analyzed the data, prepared figures and/or tables, authored or reviewed drafts of the article, and approved the final draft.
- Samuel Atcherson conceived and designed the experiments, performed the experiments, analyzed the data, prepared figures and/or tables, authored or reviewed drafts of the article, and approved the final draft.
- Jeffrey Padberg conceived and designed the experiments, performed the experiments, analyzed the data, prepared figures and/or tables, authored or reviewed drafts of the article, and approved the final draft.

Animal Ethics

The following information was supplied relating to ethical approvals (*i.e.*, approving body and any reference numbers):

The UCA IACUC Committee approved of the research in this study. All work in this study also followed USDA guidelines.

Data Availability

The raw ABR data files from the clinical Biologic Navigator Pro ABR system are available in the Supplemental File.

Supplemental Information

Supplemental information for this article can be found online at http://dx.doi.org/10.7717/peerj.16602#supplemental-information.

REFERENCES

Atcherson S, Stoody T. 2012. *Auditory electrophysiology, a clinical guide*. New York, NY: Thieme.

Bakken TE, Jorstad NL, Hu Q, Lake BB, Tian W, Kalmbach BE, Crow M, Hodge RD, Krienen FM, Sorensen SA, Eggermont J, Yao Z, Aevermann BD, Aldridge AI, Bartlett A, Bertagnolli D, Casper T, Castanon RG, Crichton K, Daigle TL, Dalley R, Dee N, Dembrow N, Diep D, Ding S-L, Dong W, Fang R, Fischer S, Goldman M, Goldy J, Graybuck LT, Herb BR, Hou X, Kancherla J, Kroll M, Lathia K, van Lew B, Li YE, Liu CS, Liu H, Lucero JD, Mahurkar A, McMillen D, Miller JA, Moussa M, Nery JR, Nicovich PR, Niu S-Y, Orvis J, Osteen JK, Owen S, Palmer CR, Pham T, Plongthongkum N, Poirion O, Reed NM, Rimorin C, Rivkin A, Romanow WJ, Sedeño-Cortés AE, Siletti K, Somasundaram S, Sulc J, Tieu M, Torkelson A, Tung H, Wang X, Xie F, Yanny AM, Zhang R, Ament SA, Behrens MM, Bravo HC, Chun J, Dobin A, Gillis J, Hertzano R, Hof PR, Höllt T, Horwitz GD, Keene CD, Kharchenko PV, Ko AL, Lelieveldt BP, Luo C, Mukamel EA, Pinto-Duarte A, Preiss S, Regev A, Ren B, Scheuermann RH, Smith K, Spain WJ, R. White OR, Koch C, Hawrylycz M, Tasic B, Macosko EZ, McCarroll SA, Ting JT, Hongkui Zeng HK, Feng G, Ecker JR, Linnarsson S, Lein ES. 2021. Comparative cellular analysis of motor cortex in human, marmoset, and mouse. *Nature* **598**:111–119 DOI 10.1038/s41586-021-03465-8.

Berqgvist LP, Abrantes EAL, Avilla LD. 2004. The Xenarthra (mammalia) of Sao Jose de Itaborai Basin (upper Paleocene, Itaboraian), Rio de Janeiro, Brazil. *Geodiversitas* **26**:323–337.

Bruns V, Muller M, Hofer W, Heth W, Nevo E. 1988. Inner ear structure and electrophysiological audiograms of the subterranean mole rat, *Spalax ehrenbergi*. *Hearing Research* **33**:l–10 DOI 10.1016/0378-5955(88)90017-2.

Concas MP, Morgan A, Serra F, Nagtegaal AP, Oosterloo BC, Seshadri S, Heard-Costa N, Van Camp G, Fransen E, Francescatto M, Logroscino G, Sardone R, Quaranta N, Gasparini P, Girotto G. 2021. Hearing function: identification of new candidate genes further explaining the complexity of this sensory ability. *Genes* **12(8)**:1228–1243 DOI 10.3390/genes12081228.

Cone-Wesson BK, Hill KG, Liu G. 1997. Auditory brainstem response in tammar wallaby (Macropus eugenii). *Hearing Research* **105**:119–129 DOI 10.1016/s0378-5955(97)00211-6.

Delsuc F, Scally M, Madsen O, Stanhope MJ, De Jong WW, Catzeflis FM, Springer MS, Douzery EJP. 2002. Molecular phylogeny of living xenarthrans and the impact of character and taxon sampling on the placental tree rooting. *Molecular Biology and Evolution* **19**:1656–1671 DOI 10.1093/oxfordjournals.molbev.a003989.

Delsuc F, Vizcaíno SF, Douzery EJ. 2004. Influence of tertiary paleoenvironmental changes on the diversification of South American mammals: a relaxed molecular clock study within xenarthrans. *BMC Evolutionary Biology* **4**:11 DOI 10.1186/1471-2148-4-11.

Dom R, Martin GF, Fisher BL, Fisher AM, Harting JK. 1971. The motor cortex and corticospinal tract of the armadillo (Dasypus novemcinctus). *Journal of the Neurological Sciences* **14**:236–255 DOI 10.1016/0022-510X(71)90092-X.

Emerling CA, Springer MS. 2015. Genomic evidence for rod monochromacy in sloths and armadillos suggests early subterranean history for Xenarthra. *Proceedings of the Royal Society of London B: Biological Sciences* **282(1800)**:20142192 DOI 10.1098/rspb.2014.2192.

Engle JR, Tinling S, Recanzone GH. 2013. Age-related hearing loss in rhesus monkeys is correlated with cochlear histopathologies. *PLOS ONE* **8(2)**:e55092 DOI 10.1371/journal.pone.0055092.

Ferrari CC. 1998. The brain of the armadillo *Dasypus hybridus*. A general view of its most salient features. *Biocell* **22**:123–140.

Garrett A, Lannigan V, Yates NJ, Rodger J, Mulders W. 2019. Physiological and anatomical investigation of the auditory brainstem in the Fat-tailed dunnart (Sminthopsis crassicaudata). *PeerJ* **7**(1–3):e7773 DOI 10.7717/peerj.7773.

Gaudin TJ. 2003. Phylogeny of the xenarthra (mammalia). In: Fariña RA, Vizcaíno SF, Storch G, eds. *Morphological Studies in Fossil and Extant Xenarthra (Mammalia)*. Vol. 83. Frankfurt: Senckenbergiana Biologica, 1–101.

Glendenning KK, Masterton RB. 1998. Comparative morphometry of mammalian central auditory systems: variation in nuclei and form of the ascending system. *Brain, Behavior, and Evolution* **51**(2):59–89 DOI 10.1159/000006530.

Gorga MP, Kaminski JR, Beauchaine KA, Jesteadt W. 1988. Auditory brainstem responses to tone bursts in normally hearing subjects. *Journal of Speech and Hearing Research* **31**(1):87–97 DOI 10.1044/jshr.3101.87.

Heffner HE, Heffner RS. 1984. Sound localization in large mammals: localization of complex sounds by horses. *Behavioral Neuroscience* **98**(3):541–555 DOI 10.1037/0735-7044.98.3.541.

Heffner RS, Heffner HE. 1990. Hearing in domestic pigs (*Sus scrofa*) and goats (*Cabra hircus*). *Hearing Research* **48**:231–240 DOI 10.1016/0378-5955(90)90063-U.

Heffner HE, Heffner RS. 2007. Hearing ranges of laboratory animals. *Journal of the American Association for Laboratory Animal Science* **46**(1):20–22.

Heffner HE, Heffner RS. 2008. High-frequency hearing. In: Dallos P, Oertel D, Hoy R, eds. *Handbook of the Senses: Audition*. New York: Elsevier, 55–60.

Heffner HE, Heffner RS. 2014. The behavioral study of mammalian hearing. In: Popper AN, Fay RR, eds. *Perspectives on Auditory Research*. New York: Springer, 269–285.

Heffner HE, Heffner RS. 2018. The evolution of mammalian hearing. In: Bergevin C, Puria S, eds. *To the Ear and Back—Advances in Auditory Biophysics*. Melville NY: American Institute of Physics Publishing, 13000–13001.

Heffner HE, Heffner RS, Contos C, Ott T. 1994. Audiogram of the hooded Norway rat. *Hearing Research* **73**(2):244–247 DOI 10.1016/0378-5955(94)90240-2.

Heffner R, Heffner H, Masterton B. 1970. Behavioral measurements of absolute and frequency-difference thresholds in guinea pig. *Journal of the Acoustical Society of America* **49**(6):1888–1895 DOI 10.1121/1.1912596.

Heffner RS, Koay G, Heffner HE. 2020. Hearing and sound localization in cottontail rabbits, Sylvilagus floridanus. *Journal of Comparative Physiology A* **206**:543–552 DOI 10.1007/s00359-020-01424-8.

Heffner H, Masterton B. 1980. Hearing in Glires: domestic rabbit, cotton rat; feral house mouse, and kangaroo rat. *Journal of the Acoustical Society of America* **68**(6):1584–1599 DOI 10.1121/1.385213.

Hodge RD, Bakken TE, Miller JA, Smith KA, Barkan ER, Graybuck LT, Close JL, Long B, Johansen N, Penn O, Yao Z, Eggermont J, Höllt T, Levi BP, Shehata SI, Aevermann B, Beller A, Bertagnolli D, Brouner K, Casper T, Cobbs C, Dalley R, Dee N, Ding S-L, Ellenbogen RG, Fong O, Garren E, Goldy J, Gwinn RP, Hirschstein D, Keene CD, Keshk M, Ko AI, Lathia K, Mahfouz A, Maltzer Z, McGraw M, Nghi Nguyen TN, Nyhus J, Ojemann JG, Oldre A, Parry S, Reynolds S, Rimorin C, Shapovalova NV, Somasundaram S, Szafer A, Thomsen ER, Tieu M, Quon G, Scheuermann RH, Yuste R, Sunkin SM, Lelieveldt B, Feng D, Ng L, Bernard A, Hawrylycz M, Phillips JW, Tasic B, Zeng H, Jones AR,

Koch C, Lein ES. 2019. Conserved cell types with divergent features in human versus mouse cortex. *Nature* **573**:61–68 DOI 10.1038/s41586-019-1506-7.

Jewett D, Williston JS. 1971. Auditory-evoked far fields averaged from the scalp of humans. *Brain* **94(4)**:681–696 DOI 10.1093/brain/94.4.681.

Keithley EM. 2019. Pathology and mechanisms of cochlear aging. *Journal of Neuroscience Research* **98**:1674–1684 DOI 10.1002/jnr.24439.

Kirchheimer WF, Storrs EE. 1971. Attempts to establish the armadillo (*Dasypus novemcinctus*) as a model for the study of leprosy. *International Journal of Leprosy* **39(3)**:693–702.

Kozlenkov A, Vermunt MW, Apontes P, Li J, Hao K, Sherwood CC, Hof PR, Ely JJ, Wegner M, Mukamel EA, Creyghton MP, Koonin EV, Dracheva S. 2020. Evolution of regulatory signatures in primate cortical neurons at cell-type resolution. *Proceedings of the National Academy of Sciences of the United States of America* **117**:28422–28432 DOI 10.1073/pnas.2011884117.

Loughry WJ, Perez-Heydrich C, McDonough CM, Oli MK. 2013. Population dynamics and range expansion in nine-banded armadillos. *PLOS ONE* **8(7)**:e68311 DOI 10.1371/journal.pone.0068311.

Loughry WJ, Prodohl PA, McDonough CM, Avise JC. 1998. Polyembryony in armadillos: an unusual feature of the female nine-banded armadillo's reproductive tract may explain why her litters consist of four genetically identical offspring. *American Scientist* **86(3)**:274–279 DOI 10.1511/1998.3.274.

Loughry WJ, Superina M, McDonough CM, Abba AM. 2015. Research on armadillos: a review and prospectus. *Journal of Mammalogy* **96(4)**:635–644 DOI 10.1093/jmammal/gyv005.

Masterton B, Heffner H, Ravizza R. 1969. The evolution of human hearing. *Journal of the Acoustical Society of America* **45**:966–985 DOI 10.1121/1.1911574.

Mills DM, Shepherd RK. 2001. Distortion product otoacoustic emission and auditory brainstem responses in the echidna (Tachyglossus aculeatus). *Journal of the Association for Research in Otolaryngology* **2(2)**:130–146 DOI 10.1007/s101620010059.

Moffitt TB. 2015. The effective frequency range and auditory sensitivity of dasypus novemcinctus. Master's thesis. University of Central Arkansas.

Moller-Krull M, Delsuc F, Churakov G, Marker C, Superina M, Brosius J, Douzery EJP, Schmitz J. 2007. Retroposed elements and their flanking regions resolve the evolutionary history of xenarthran mammals (armadillos, anteaters, and sloths). *Molecular Biology and Evolution* **24(11)**:2573–2582 DOI 10.1093/molbev/msm201.

Moraes-Barros N, Arteaga MC. 2015. Genetic diversity in Xenarthra and its relevance to patterns of neotropical biodiversity. *Journal of Mammalogy* **96(4)**:690–702 DOI 10.1093/jmammal/gyv077.

Morgan C, Foster PG, Webb A, Pisani D, McInerney JO, O'Connell M. 2013. Heterogeneous models place the root of the placental mammal phylogeny. *Molecular Biology and Evolution* **30**:2145–2156 DOI 10.1093/molbev/mst117.

Muller M, Burda H. 1989. Restricted hearing range in a subterranean rodent, *Cryptomys hottentotus*. *Naturwissenschaften* **76**:134–135 DOI 10.1007/BF00366611.

Oliveira EV, Bergqvist LP. 1998. A new paleocene armadillo (Mammalia, Dasypodoidea) from the Itaboraí Basin, Brazil. In: *Paleógeno de América del Sur y de la Península Antártica*. Vol. 5 Asociación Paleontológica Argentina, 35–40.

Padberg J. 2017. Xenarthran nervous systems. In: Kaas J, ed. *Evolution of Nervous Systems 2e*. Vol. 2. Oxford: Elsevier, 383–412.

Peterson EA, Heaton WC. 1968. Peripheral auditory responses in representative edentates. *Journal of Auditory Research* **8(2)**:171–181.

Powers BE, Widholm JJ, Lasky RE, Schantz SL. 2006. Auditory deficits in rats exposed to an environmental mixture during development. *Toxicological Sciences* **89(2)**:415–422 DOI 10.1093/toxsci/kfj051.

Recanzone G. 2018. The effects of aging on auditory cortical function. *Hearing Research* **366**:99–105 DOI 10.1016/j.heares.2018.05.013.

Reimer K. 1995. Hearing in the marsupial *Monodelphis domestica* as determined by auditory-evoked brainstem responses. *Audiology* **34**:334–342 DOI 10.3109/00206099509071923.

Reimer K. 1996. Ontogeny of hearing in the marsupial, *Monodelphis domestica*, as revealed by brainstem auditory evoked potentials. *Hearing Research* **92**:143–150 DOI 10.1016/0378-5955(95)00213-8.

Ridgway SH, Bullock TH, Carder DA, Seeley RL, Woods D, Galambos R. 1981. Auditory brainstem response in dolphins. *Proceedings of the National Academy of Sciences of the United States of America* **78(3)**:1943–1947 DOI 10.1073/pnas.78.3.1943.

Royce GJ, Martin G. 1975. Functional localization and cortical architecture in the nine-banded armadillo (*Dasypus novemcinctus mexicanus*). *The Journal of Comparative Neurology* **164(4)**:495–521 DOI 10.1002/cne.901640408.

Scholl B, Rylee J, Luci J, Priebe N, Padberg J. 2017. Orientation selectivity in the visual cortex of the nine-banded armadillo. *Journal of Neurophysiology* **117(3)**:1395–1406 DOI 10.1152/jn.00851.2016.

Scillato-Yané GJ. 1976. Dasypodidae from Riochican of Itoboraí (Brazil). *Anais da Academia Brasileira de Ciencias* **48**:527–530.

Sharma R, Lahiri R, Scollard DM, Pena M, Williams DL, Adams LB, Figarola J, Truman RW. 2013. The armadillo: a model for the neuropathy of leprosy and potentially other neurodegenerative diseases. *Disease Models and Mechanisms* **6**:19–24 DOI 10.1242/dmm.010215.

Sharma R, Singh P, Loughry WJ, Lockhart JM, Inman WB, Duthie MS, Pena MT, Marcos LA, Scollard DM, Cole ST, Truman RW. 2015. Zoonotic leprosy in the southeastern United States. *Emerging Infectious Diseases* **21(12)**:2127–2134 DOI 10.3201/eid2112.150501.

Simpson G. 1931. Metacheiromys and the Edentata. *Bulletin of the American Museum of Natural History* **59**:295–381.

St. Jules RS. 1984. The retina of the nine-banded armadillo (Dasypus novemcinctus). Doctoral Dissertation, Texas A&M University, College Station, TX, USA.

Stapells DR. 2000. Threshold estimation by the tone-evoked auditory brainstem response: a literature meta-analysis. *Journal of Speech-Language Pathology and Audiology* **24(2)**:74–83.

Stehli FG, Webb SD. 1985. *The Great American Biotic Interchange*. New York, London: Plenum Press.

Suga N. 1967. Hearing in some arboreal edentates in terms of cochlear microphonics and neural activity. *Journal of Auditory Research* **7**:267–270.

Superina M, Loughry WJ. 2015. Why do xenarthrans matter? *Journal of Mammalogy* **96(4)**:617–621 DOI 10.1093/jmammal/gyv099.

Teeling EC, Jones G, Rossiter SJ. 2016. Phylogeny, genes, and hearing: implications for the evolution of echolocation in bats. In: Fenton M, Grinnell A, Popper A, Fay R, eds. *Bat Bioacoustics, Springer Handbook of Auditory Research*. Vol. 54. New York, NY: Springer DOI 10.1007/978-1-4939-3527-7_2.

Tosches MA, Laurent G. 2019. Evolution of neuronal identity in the cerebral cortex. *Current Opinion in Neurobiology* **56**:199–208 DOI 10.1016/j.conb.2019.04.009.

Truman RW, Singh P, Sharma R, Busso P, Rougemont J, Paniz-Mondolfi A, Kapopoulou A, Brisse S, Scollard DM, Gillis TP, Cole ST. 2011. Probably zoonotic leprosy in the southern United States. *New England Journal of Medicine* **364**:1626–1633 DOI 10.1056/NEJMoa1010536.

Tuebenbacher U, Doss GA, Guevar J. 2020. Brainstem auditory-evoked response in healthy African pygmy hedgehogs (*Atelerix albiventris*). *Journal of Small Animal Practice* **62**:49–54 DOI 10.1111/jsap.13264.

Vizcaino SF, Bargo MS. 2014. Loss of ancient diversity of xenarthrans and the value of protecting extant armadillos, sloths, and anteaters. *Edentata* **15**:27–38 DOI 10.5537/020.015.0111.

Vizcaino SF, Bargo MS, Farina RA. 2008. Form, function, and paleobiology in xenarthrans. In: Vizcaino SF, Loughry WJ, eds. *The Biology of the Xenarthra*. Gainesville: University Press of Florida.

Wang H, Zhao H, Chu Y, Feng J, Sun K. 2021. Assessing evidence for adaptive evolution in two hearing-related genes important for high-frequency hearing in echolocating mammals. *G3 Genes|Genomes|Genetics* **11(4)**:1–12 DOI 10.1093/g3journal/jkab069.

Webb SD. 1976. Mammalian faunal dynamics of the great American interchange. *Paleobiology* **2(3)**:220–234 DOI 10.1017/S0094837300004802.

Wilson WJ, Mills PC. 2005. Brainstem auditory-evoked response in dogs. *American Journal of Veterinary Research* **66(12)**:2177–2187 DOI 10.2460/ajvr.2005.66.2177.

Wirthlin ME, Johansen NJ, Jorstad NL, Yanny AM, de Sousa AA, Bertagnolli D, Chakka AB, Chakrabarty R, Ding S-L, Ferrer R, Goldy J, Guilford N, Guzman J, Hirschstein D, Omstead V, Pham T, Rimorin C, Seeman S, Shapovalova NV, Taskin N, Tieu M, Torkelson A, Weed N, Balmus G, Barrett T, Bolser D, Drew K, Fitzpatrick D, Freeman SM, Halley A, Horwitz GD, Kaas J, Kojima Y, Krasnow M, Krubitzer L, Levi BP, Padberg J, Ting JT, Ungerliden K, Wilkerson GK, Yartsev M, Lelieveldt BP, Sherwood CC, Smith K, Hodge RD, Lein ES, Bakken TE. 2023. Transcriptomic and epigenomic data for 26 species provide insight into the evolution of mammalian motor cortex, Online. In: *Program Number PSTR490.11. 2023 Neuroscience Meeting Planner*. Washington, D.C.: Society for Neuroscience. *Available at* https://www.abstractsonline.com/pp8/#!/10892.

Yanny A, Jorstad N, Bakken T, Hodge R, Smith K, Goldy J, Guildord J, Guzman J, Pham T, Torkelson A, Chakrabarty R, Hirchstein D, Shapovalova N, Barlow S, Yellowhair T, Barrett T, Englund M, Krubitzer L, Padberg JJ, Stimpson C, Sherwood C, Goropashnaya A, Federov V, Drew K, Wilkerson G, Lein E. 2021. Analysis of primary motor cortex across diverse mammalian species reveals divergent cell type features. In: *Program Number P915.09. 2021 Neuroscience Meeting Planner*. Chicago, IL: Society for Neuroscience. *Available at* https://www.abstractsonline.com/pp8/#!/10485.